

Co-combustion performance analysis of a Fujian anthracite with *Cunninghamia lanceolata* and Mycorrhizal plants

Progress in Reaction Kinetics

and Mechanism

Volume 46: 1–12

© The Author(s) 2021

Article reuse guidelines:

sagepub.com/journals-permissions

DOI: 10.1177/14686783211010966

journals.sagepub.com/home/prk



Zheng Zou, Yangui Chen^{ID}, Jieqing Zheng^{ID},
Xiaodong Zhang and Hongzhou He

Abstract

The co-combustion characteristics of Fujian anthracite with two biomasses (i.e. *Cunninghamia lanceolata*) and Mycorrhizal plants in different proportions were investigated using thermogravimetric analysis. The result showed that first, the co-combustion processes of Fujian anthracite with the two biomasses (*Cunninghamia lanceolata* and Mycorrhizal plants) proceeded in three stages, separation and combustion of volatiles, combustion of fixed carbon in the biomass, and combustion of fixed carbon in Fujian anthracite. Secondly with increasing proportion of biomass, the co-combustion of Fujian anthracite with *Cunninghamia lanceolata* and Mycorrhizal plants shifted to a low-temperature zone, with a lower ignition temperature, shortened burnout time, and growth of both combustibility index (C_i) and comprehensive combustion index S . Finally, at different mixing proportions, the comprehensive combustion index S during co-combustion of FW with Mycorrhizal plants is always larger than that during co-combustion with *Cunninghamia lanceolata*; therefore, FW and Mycorrhizal plants exhibit superior comprehensive co-combustion performance to FW and *Cunninghamia lanceolata*. Analysis of various parameters pertaining to combustion performance shows that the ignition and combustion performance of Fujian anthracite was improved as long as the Fujian anthracite was mixed with around 20% biomass.

Keywords

Fujian anthracite, biomass, co-combustion, thermogravimetric analysis

School of Mechanical and Energy Engineering, Jimei University, Xiamen, P.R. China

Corresponding author:

Jieqing Zheng, School of Mechanical and Energy Engineering, Jimei University, Xiamen 361021, P.R. China.

Email: zhengjieqing@jmu.edu.cn



Creative Commons Non Commercial CC BY-NC: This article is distributed under the terms of the Creative Commons Attribution-NonCommercial 4.0 License (<https://creativecommons.org/licenses/by-nc/4.0/>) which permits non-commercial use, reproduction and distribution of the work without further permission provided the original work is attributed as specified on the SAGE and Open Access pages (<https://us.sagepub.com/en-us/nam/open-access-at-sage>).

Introduction

As a renewable energy source, biomass can be transformed into three-phase (gas, liquid, and solid) fuel.¹ Biomass can be easily ignited due to its highly volatile nature, low ash content, and low sulfur content and is thus regarded as a renewable, environmentally friendly, sustainable source of clean energy. Effective development and clean utilization of biomass resources is important on a global scale.²⁻⁴ Direct combustion technology for biomasses shows significant environmental benefits. Despite this, black smoke is likely to be emitted and tarry substances are deposited on the heated surface during direct combustion of biomass in a boiler, as the material has a high moisture content and a high alkali metal content in the resulting ash, thus leading to coking and alkaline corrosion; moreover, biomass is unevenly distributed and has a low energy density. Thus, the pre-treatment cost for biomass burning is high and the cost for simple biomass burning is higher than that for conventional energy. Besides, it is difficult to guarantee the sustainable supply of such fuels. In addition, the combustion efficiency and boiler thermal efficiency are both low, which hinders the efficient utilization of biomass fuels.

The co-combustion of biomass and coal is regarded as an energy utilization strategy suited to full use of coal and biomass resources. It can address the deficiencies occurring during single biomass combustion and also reduce pollution generated by coal combustion, thus protecting the environment and realizing the comprehensive utilization of fossil energy and renewable energy.⁵ Huang et al.⁶ experimentally investigated co-pyrolysis of bituminous coal and biomass in a pressurized fluidized bed reactor: the results show that co-pyrolysis of bituminous coal and biomass presents a synergistic effect and the addition of biomass influences the yield of tar and coke and the compositions of gases and tars during co-pyrolysis. By measuring the co-pyrolysis performance of sawdust and coal in a fixed bed reactor, Park et al.⁷ found that the yields and conversion rates of sawdust and coal during co-pyrolysis are both higher than those during single pyrolysis. In terms of volatiles, Alobaid et al.⁸ conducted the co-combustion of biological residues treated at a high temperature and hard coal in a pulverized coal boiler rated at 1 MW_{th}. Compared with only burning hard coal, more volatile matters were released from positions close to the burner, thus generating a higher demand for oxygen. Konwar et al.⁹ assessed the effect of the addition of biomass on pyrolytic behaviors of low-rank bituminous coal using thermogravimetric analysis (TGA). The result indicated that coal interacts with biomass residues and the synergistic effect is related to the rate of heating, relative proportions of coal and biomass, and the chemical compositions thereof. Other reports also suggest that the mix proportions, rate of heating, and so on will influence the products and behaviors of co-pyrolysis of coal and biomass.¹⁰⁻¹⁴ Guo et al.¹⁵ compared the co-combustion performance of biomass particles with bituminous coal and Xiaolongtan lignite using TGA. The result showed that the maximum combustion rate and combustion index increase while the burnout temperature decreases with an increase in the proportion of biomass. This indicated that the combustion performance of coal is improved. Moreover, the interaction between biomass particles and Xiaolongtan lignite is more significant than that between biomass particles and bituminous coal. Toptas et al.¹⁶ investigated the combustion behavior of lignocellulosic and animal waste and the blends with lignite. The results indicated that biomass addition can improve the burnout performance of lignite, and the blends have a lower ignition and burnout temperature at 50% coal. Wang et al.¹⁷ investigated the co-combustion of coal and biomass (sawdust and rice straw): it was found that there was a certain interaction between the coal and the biomass. Ignition and burnout temperatures

decrease with increasing biomass ratio. Using TGA, it is also verified that there is a synergistic effect in the combustion process of biomasses and coal and increasing the amount of added biomass can improve the ignition performance and thermal reactivity of coal.^{18–21} Guo and Zhong²² conducted research into the co-combustion of anthracite and sawdust particles in a fluidized bed and studied thermodynamic behaviors arising during co-combustion of the two through TGA. Research results indicated that co-combustion of the two facilitates combustion and reduces emissions of gaseous pollutants (such as SO₂ and NO). In addition, the clinkering rate of ashes in the sawdust can be decreased by co-combustion with coal. Based on a pilot-scale coal-fired power plant, Yelverton et al.²³ mixed four different types of woody biomass with coal, separately, at the mass ratios of 20% and 40% to measure the composition and particle size distribution of tail gases. Wang et al.²⁴ explored the release and conversion of arsenic (As) separately after co-combustion of tobacco stem, black bean straw, wheat straw, millet straw, corn stalk, and rice straw with coal. Except for rice straw, which can promote the release of As, the other biomass materials all inhibit the release of As. Chen et al.²⁵ studied the NO_x and SO₂ emission characteristics during co-combustion of anthracite and refuse-derived fuel in a precalciner.

Only a single variety of coal resources is available in Fujian Province, China: this resource has a high carbon content and caloric value; however, the majority of the coal is Class-II anthracite with a volatile content of 2%–4%, which is difficult to ignite and burn out. The thermal efficiency of the Class-II anthracite remains low even during combustion in a circulating fluidized bed boiler which is widely applicable to the different types of coal encountered in practical application. Zhuang et al.²⁶ compared the combustion performance of superfine Fujian anthracite (FA) by performing TGA on superfine FA and conventional FA. The result revealed that super-fining confers a more positive effect in inhibiting deficiencies (such as difficulty in ignition, poor stability, and imperfect combustion) of FA. Jaffri and Zhang²⁷ explored CO₂ gasification in FA under ambient pressure at 750°C to 950°C by taking black liquor as the catalyst based on TGA. During co-combustion of FA and biomass, the ignition and combustion performance can be optimized by utilizing the complementary action between high content of volatiles in the added biomass and the high calorific value of FA.

Mycorrhizal plants (also called as Juncos, JC) refer to herbaceous plants that can be used as culture media for edible and medicinal mushrooms and have comprehensive development and utilization value. JC is characterized by a developed root system, rapid growth, high yield, and less stringent requirements demanded of the soil.²⁸ Lin et al.²⁹ investigated the use of JC during growth for 3 months, 1 year, and 2 years as a biomass fuel. They found that JC growing for different periods could achieve a calorific value of about 68.2%–86.9% of that of raw coal; therefore, JC may be used as a biomass fuel. *Cunninghamia lanceolata* (CL) is commercial tree species that is widely planted in southern China, and it grows rapidly and is of high economic value.

Above all, many in-depth studies on the co-pyrolysis and co-combustion of biomass and coal have been reported and the ignition and combustion performance can be analyzed and compared using TGA. The reaction mechanism between coal and biomass has not yet been elucidated; moreover, owing to coal and biomass resources exhibiting certain regional characteristics, these are divided into different types and therefore have distinct fuel characteristics, such that significant differences are manifest in their subsequent co-combustion processes. Therefore, the co-combustion tests of FA having ultra-low volatiles with two types of added biomass, that is, CL and JC, were conducted using a thermogravimetric

Table 1. Ultimate and proximate analysis of samples (wt. %).

Specimen	Ultimate analysis (wt. %)					Proximate analysis (wt. %)			
	N _{ad}	C _{ad}	H _{ad}	S _{ad}	O _{ad}	A _{ad}	M _{ad}	V _{ad}	FC _{ad}
FA	0.54	63.84	1.20	0.91	3.58	25.61	4.32	4.22	65.85
CL	0.15	49.90	4.60	0.04	29.72	0.84	14.23	70.61	13.02
JC	0.33	40.10	4.55	0.17	38.51	6.89	6.58	65.96	15.74

ad: air dry; A: ash; M: moisture; V: volatile matter; FC: fixed carbon; FA: Fujian anthracite; CL: *Cunninghamia lanceolata*; JC: Mycorrhizal plants.

analyzer. Furthermore, the ignition and combustion performance during co-combustion of blends with different constituent proportions was analyzed and compared. The research results are expected to provide valuable reference for co-combustion of FA and biomass in a boiler.

Samples and methods

Samples

FA was used as the coal samples while woody CL sawdust and herbal JC particles were taken as biomass specimens. Various test specimens were prepared through a series of pre-treatments including crushing and drying. The ultimate and proximate analyses were conducted on the samples using a Vario MICRO elemental analyzer and a 5E-MAG6700/6600B proximate analysis instrument (Table 1).

Test conditions and process

The METTLER TGA/DSC1/1600LF thermogravimetric analyzer was applied during the test. The test was conducted in air at a flow rate of 60 mL/min, a heating rate of 100°C/min, over a temperature range from room temperature to 1200°C, and using specimens with a mass of 5 ± 0.5 mg.

The TGA tests were conducted on separate combustion and co-combustion of coal samples and biomasses. In terms of co-combustion, the TGA tests were separately performed after uniformly mixing biomass with coal in the mass ratios of 1:1, 1:2, 1:3, and 1:5 (with corresponding mass percentages of biomass of 50%, 33%, 25%, and 17%, respectively). It was important to ensure that the experimental results had good reproducibility, so each test was repeated at least twice before a final result was ascertained.

Parametric determination of combustion performance

In this study, the first steep peak region with obvious weight loss on the DTG curve was taken as the region of ignition and stable combustion, and the ignition temperature T_i was determined using the TG/DTG tangent method,¹⁵ that is, after drawing a perpendicular line through this peak on the DTG curve to intersect the TG curve, a tangent to the TG curve is drawn across the point of intersection. The corresponding temperature at the intersection

between the tangent and the flat straight line when weight loss starts to occur on the TG curve is defined as the ignition temperature T_i ; the burnout temperature T_h corresponds to the point with the mass loss rate of $-1\%/min$ in the zone at the end of combustion on the DTG curve.

The combustion performance of samples in the early period was analyzed and compared using the combustibility index (C_i).^{30,31} The index is a discriminative index proposed by Xi'an Thermal Power Research Institute Co., Ltd and is used for determining ignition and combustion stability. Yang et al.³¹ found that the value of C_i increases with the increasing biomass content.

The greater the value of C_i , the better the ignition and combustion stability. C_i is given by Formula (1)

$$C_i = DTG_{\max} / T_i^2 \quad (1)$$

where DTG_{\max} denotes the maximum rate of combustion and T_i refers to the ignition temperature.

To evaluate the combustion performance of samples, the test results were analyzed by utilizing the comprehensive combustion index S for combustion performance. The value of S reflects the ignition and combustion performance of the specimens.^{15,17,19,21} The greater the value of S , the better the combustion performance. The value of S is given by Formula (2)

$$S = \frac{DTG_{\max} DTG_{\text{mean}}}{T_i^2 T_h} \quad (2)$$

where DTG_{mean} and T_h represent the average combustion rate and burnout temperature, respectively.

Results and analysis

Analysis of fuel characteristics

It can be seen from Table 1 that the two biomasses show lower ash, nitrogen, and sulfur contents than FA, which hints at the clean combustion characteristic of such types of biomass. Moreover, the two biomasses also contain a high volatile matter content (those in CL and JC are about 16.7 and 15.6 times that in FA, respectively); moreover, the ratio of volatiles to fixed carbons is also high (about 4.2 and 5.4 in JC and CL, respectively), indicative of greater ease of ignition. In addition, biomass samples contain more hydrogen and oxygen than samples of FW, indicating that biomass has a higher reactivity and is easier to ignite.^{19,22} Thus, it is feasible to enhance the ignition and combustion characteristics by adding biomass to the coal.

In addition, biomass mainly consists of cellulose, hemicellulose, and lignin, in which hemicellulose is the least stable and shows the highest reactivity while lignin delivers the optimal stability among the three. Generally, the lignin content of woody biomass is higher than that in herbal biomass; therefore, by comparing the two biomasses (CL and JC), the reactivity of herbal JC is found to be better; moreover, JC is drier than CL while having a higher oxygen content, which is also conducive to ignition and combustion.

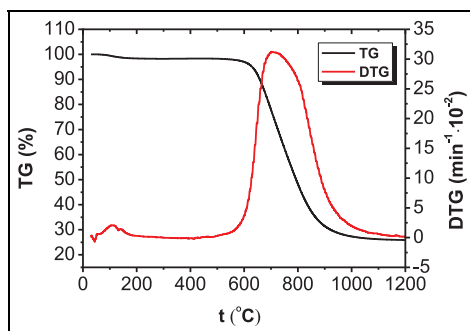


Figure 1. TG and DTG curves of FA.

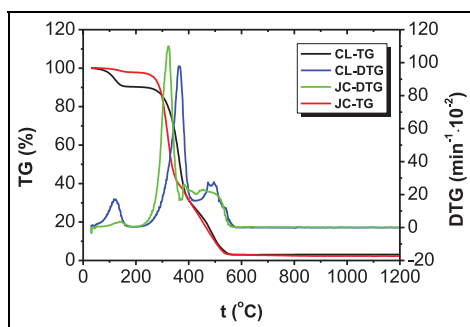


Figure 2. TG and DTG curves of CL and JC.

Separate combustion processes of FA and biomasses

Figures 1 and 2 separately illustrate the TG and DTG curves during separate combustion of FA and the two biomasses (CL and JC).

As shown in Figure 1, the DTG curve of FA contained a peak at about 600°C–900°C caused by the combustion of the fixed carbons owing to the volatile content therein only accounting for 4.22% by mass. This meant that FA would deliver a low oxidation rate within a wide temperature range, so it was difficult for FA to undergo ignition and combustion reactions. It can be seen from Figure 2 that there are three peaks on the DTG curves corresponding to the combustion processes of the two types of biomass (CL and JC): the first peak appeared at between 50°C and 150°C in the dehydration and drying stage; the second peak was found at between 200°C and 400°C and arose due to the separation and combustion of volatiles; the third peak was induced by the combustion of cokes as a product of biomass pyrolysis, which occurred between 400°C and 600°C. There were significant weight-loss peaks on the DTG curves of biomasses separately caused by combustion of volatiles and carbons; however, the former (the peak caused by combustion of volatiles) was generally far larger than the latter (the peak induced by the combustion of carbons) because the volatile content was higher than the content of fixed carbons in the two types of biomasses. In addition, compared with anthracite, the peak corresponding to the maximum rate of combustion

Table 2. Combustion characteristic parameters during single combustion of FA, CL, and JC.

Samples	T_i (°C)	T_h (°C)	T_{max} (°C)	DTG _{max} (%/min)	DTG _{mean} (%/min)	$S \times 10^7$	$C_i \times 10^6$
FA	642.10	803.49	710.31	31.29	7.16	6.77	2.14
CL	310.27	575.56	361.47	97.96	17.96	317.46	17.57
JC	275.72	566.02	317.70	110.02	18.34	468.97	19.95

FA: Fujian anthracite; CL: *Cunninghamia lanceolata*; JC: Mycorrhizal plants.

of biomass occurred within a low-temperature zone and the peak was narrow, high, and steep, which implied that its corresponding volatiles were separated and burned, suggesting an intense combustion reaction. In contrast, owing to afterburning of FA, the peak of the maximum combustion rate was found in a high-temperature zone with fixed carbon combustion. In this case, the peak covered a wide temperature range and was shallower and broader.

Table 2 lists the main performance parameters measured during separate combustion of coal samples and two types of biomasses. It can be seen from the data in Table 2 that the combustion performance parameters of CL and JC during separate combustion are insignificantly different. Although the volatile content in CL was higher than that in JC, the ignition and burnout temperatures of JC were both lower than those of CL while its maximum combustion rate $(dm/dt)_{max}$ and average combustion rate $(dm/dt)_{mean}$ were higher than those of CL. Correspondingly, according to the DTG curves in Figure 2, the peak attributed to separation and combustion of the volatiles in JC was steeper, implying that JC was more easily ignited and more intensely combusted, showing a better combustion performance than CL. This result was also verified using the values of C_i and S . In the process of separate combustion, the ignition temperature of FA was 331.83°C higher than that of CL and 366.38°C higher than that of JC; moreover, the burnout temperature of FA was 228.34°C higher than that of CL and 237.38°C higher than that of JC; however, the maximum combustion rate $(dm/dt)_{max}$ and the average combustion rate $(dm/dt)_{mean}$ of FA were both about three times lower than those of the two types of biomasses. In addition, the C_i value of FA was only about 11% of that of the two types of biomasses while its S value showed a difference of 50–70 times that of the two types of biomasses. This indicated that FA was harder to ignite and burn out owing to the volatile content therein being much lower than that in the biomass.

Co-combustion process of FA and biomasses

A comparison of TG and DTG curves at different biomass contents was made by processing the test data on co-combustion of FA with CL and JC mixed in different proportions (Figures 3 and 4).

As shown in Figures 3 and 4, four weight-loss peaks appeared on the DTG curves attained after co-combustion of FA with the two types of biomasses (CL and JC). The first peak at 50°C–200°C was formed due to dehydration; the second peak occurring at 200°C–400°C was caused by separation and combustion of volatiles in the biomass. In this stage, the cellulose underwent pyrolysis to generate volatiles which burned fiercely; the third weight-loss peak was triggered by the combustion of fixed carbons in the biomass, as seen between 400°C and 600°C; the fourth weight-loss peak at 600°C–800°C was a result of the combustion of fixed carbons in FA. The second and the fourth peaks were the most significant and the overall

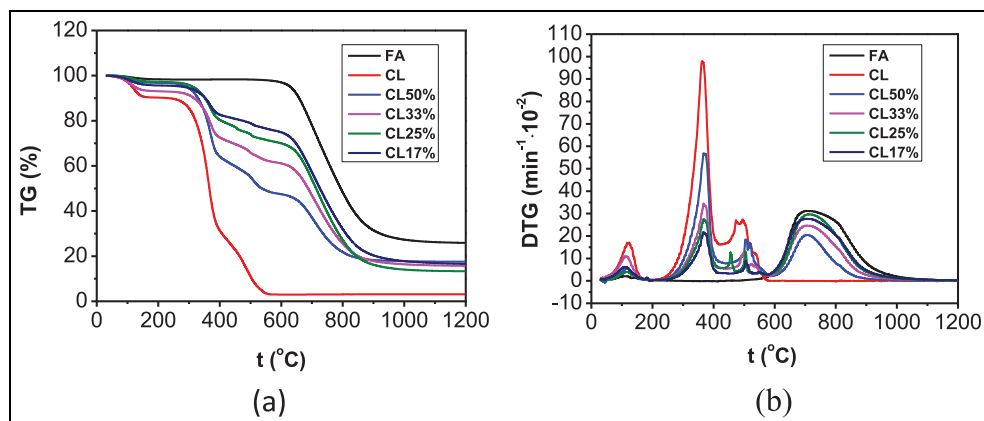


Figure 3. (a) TG and (b) DTG curves during co-combustion of FA with different CL contents.

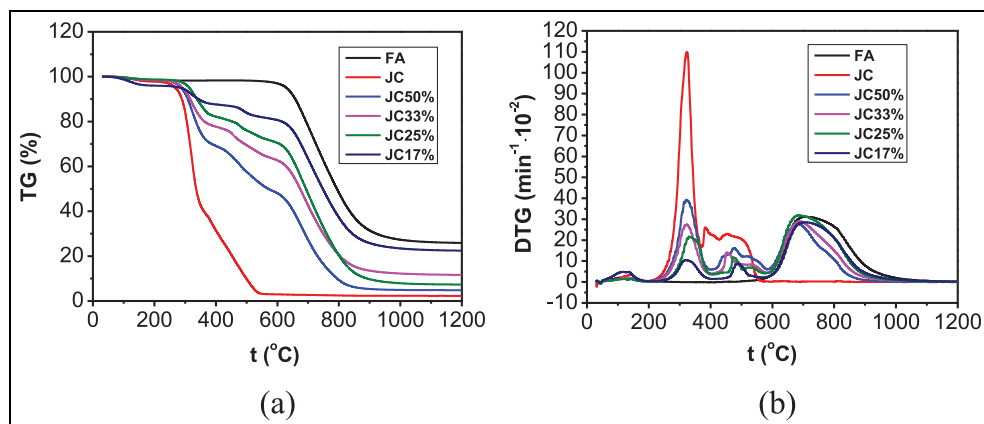


Figure 4. (a) TG and (b) DTG curves during co-combustion of FA with different JC contents.

weight loss curves reflected the superposition of separate combustion processes of biomass and FA. It can also be found from the figures that when the proportion of biomass was low, the second peak with its larger temperature range was broader and shallower. However, the TG curves shifted to the low-temperature zone with increasing biomass content. In this case, the second peak became steeper, narrower, and increased in amplitude. Moreover, the fourth peak was also shifted to a low-temperature zone and it declined in amplitude. This result showed that, with increasing biomass content, the volatile content increased and therefore volatiles were better separated and combusted, which was conducive to ignition. In this context, the combustion reaction appeared early in the process and the burnout time decreased.

Table 3 lists the main performance parameters during co-combustion of FA with CL and JC blended in different proportions, the ignition temperature (decreasing from 642.1°C to about 300°C) of the co-combustion of FA with these types of biomasses decreased compared with that during separate combustion, which approximated to the ignition temperature

Table 3. Combustion performance parameters during co-combustion of FA with CL and JC.

Samples	T_i (°C)	T_h (°C)	T_{max} (°C)	DTG _{max} (%/min)	DTG _{mean} (%/min)	$S \times 10^7$	$C_i \times 10^6$
CL50%	336.88	806.55	366.61	56.92	9.36	58.18	7.90
CL33%	337.13	803.48	364.76	35.10	8.75	33.64	5.07
CL25%	338.43	803.20	718.64	29.74	8.82	28.51	4.27
CL17%	343.97	798.85	707.90	27.68	8.26	24.20	4.17
JC50%	292.73	803.00	315.07	39.66	10.88	62.69	6.06
JC33%	293.74	799.50	695.24	29.12	9.353	39.48	4.40
JC25%	309.75	799.95	684.87	32.01	9.582	39.97	4.57
JC17%	312.38	799.86	706.84	28.59	7.76	28.41	4.95

FA: Fujian anthracite; CL: *Cunninghamia lanceolata*; JC: Mycorrhizal plants.

during separate combustion of each type of biomass. Moreover, the temperature corresponding to the maximum rate of combustion also decreased, which implied that the addition of biomass improved the ignition performance of FA. The reason for this was that a large amount of volatiles were contained in the biomass and they were separated out at a low temperature, thus promoting ignition and combustion. It can also be seen from Table 3 that the ignition temperature started to slowly decrease with increasing biomass content. The ignition temperatures during co-combustion dropped from 337.12°C to 336.88°C when the contents of CL and JC were increased from 33% to 50%. The average combustion rate $(dm/dt)_{mean}$ during co-combustion increased relative to that during separate combustion of FA and the burnout temperature was similar to that during separate combustion of FA because the burnout temperature was mainly dependent on the combustion of fixed carbons; however, the amount of fixed carbons in these two types of biomasses was much lower than that in FA. Thus, the burnout temperature during co-combustion approximated to that during separate combustion of FA.

Comparative analysis of combustion performance

The relationships of C_i and S with the biomass content in the co-combustion process of FA with CL and JC are demonstrated in Figures 5 and 6. The C_i (2.142×10^{-6} mg/(min·°C²)) and S (6.765×10^{-7} %²/(min²·°C³)) during separate combustion of FA were the lowest. As the biomass content increased, the values of C_i and S both increased. It can be seen from the figure that when the biomass content was below 17%, the values of C_i and S during co-combustion of FW and biomasses both increased to a significant extent. However, when the biomass content was between 17% and 33%, the increase in values of C_i and S diminished, especially in the case of the value of C_i during co-combustion of FW and JC (it even declined slightly within that interval). This is because the ash content in the biomass has certain influences on the combustion.³¹ Due to the extremely low volatile content in FW, the early stage of the co-combustion mainly involved the combustion of volatiles and fixed carbons in the biomass, and the large ash content produced in the process blocks capillary pores in the fuel. This hinders the further separation and combustion of volatiles. The value of C_i was used to characterize the combustion performance of samples in the early stage. As JC has a higher ash content than CL, the value of C_i in the co-combustion of JC with FW was lower than that in the co-combustion of CL with FW at biomass contents exceeding 33%. When the

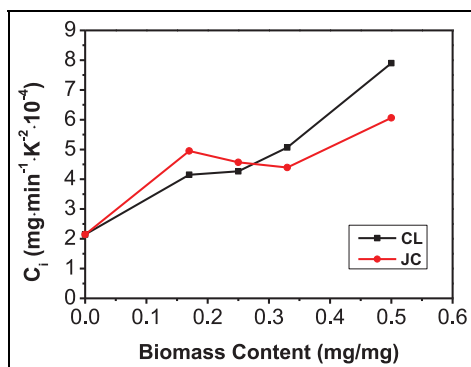


Figure 5. Relationships between C_i and the biomass content during co-combustion of FA with CL and JC.

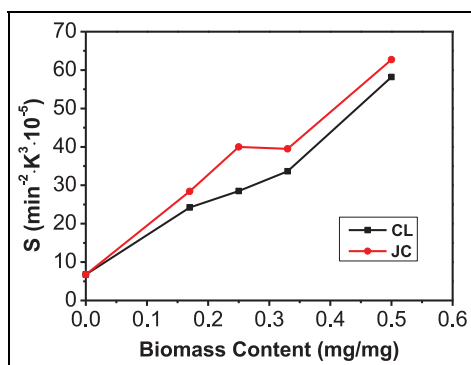


Figure 6. Relationships between S and the biomass content during co-combustion of FA with CL and JC.

biomass content was increased to greater than 33%, the release of volatiles, and the combustion reaction, intensified due to the significant increase in the amount of volatile compounds present, resulting in significant increments in values of C_i and S in co-combustion of FW with CL and with JC. It can also be seen from Figure 6 that the value of the comprehensive combustion index S in co-combustion of FW with JC (in different mix proportions) is always greater than that with CL. This is because compared with CL, JC contains more fixed carbon and oxygen, and its values of C_i and S are both larger than those of CL when combusted alone. This explains why JC exhibits the better comprehensive ignition and combustion performance.

Conclusion

First, the separate combustion process of FA differed from co-combustion processes of FA with two types of biomasses (CL and JC). The ignition temperature of FA is about 350°C higher than that of each of the two types of biomasses while its burnout temperature is about

250°C higher. The C_i of FA is only about 11% of that of the two types of biomasses while its S value differs by about 50–70 times compared with that of the biomass.

Second, with the increase in the proportion of biomass, the co-combustion reaction of FA with the two types of biomasses (CL and JC) was shifted to a low-temperature zone, with the reduction of ignition temperature, early combustion, shortened burnout time, and both growth of C_i and S . As a result, the ignition and combustion performance of FA can be improved.

Third, at different mixing proportions, the comprehensive combustion index S during co-combustion of FW with JC is always larger than that during co-combustion with CL, so FW and JC exhibit superior comprehensive co-combustion performance to FW and CL.

Finally, by analyzing various combustion performance parameters, the ignition and combustion performance of FA can be improved when biomass was mixed with FA to a proportion of about 20% by mass. If the biomass contents were to be increased further, a series of problems (such as low calorific value, coking, and alkaline corrosion) could occur during practical application. Therefore, it was advised to set the added amount of biomass to 20%.

Acknowledgements

This research work has been conducted at Jimei University.

Declaration of conflicting interests


The author(s) declared no potential conflicts of interest with respect to the research, authorship, and/or publication of this article.

Funding

The author(s) disclosed receipt of the following financial support for the research, authorship, and/or publication of this article: The authors acknowledge the financial support received from the National Natural Science Foundation of China (Project No. 51876108) and Jimei University (Project No. ZP2020053) of China.

ORCID iDs

Yangui Chen  <https://orcid.org/0000-0001-7783-3527>

Jieqing Zheng  <https://orcid.org/0000-0002-2299-489X>

References

1. Mao G, Huang N, Chen L, et al. *Sci Total Environ* 2018; 635: 1081–1090.
2. Yan P, Xiao C, Xu L, et al. *Renew Sustain Energy Rev* 2020; 127: 109857.
3. Sulaiman C, Abdul-Rahim AS and Ofozor CA. *J Clean Prod* 2020; 253: 119996.
4. Wang Z, Bui Q and Zhang B. *Energy* 2020; 194: 116906.
5. van Loo S and Koppejan J. *Handbook of Biomass Combustion and Co-firing*. Netherland: Twente University Press, 2002.
6. Huang Y, Wang N, Liu Q, et al. *Chin J Chem Eng* 2019; 27: 1666–1673.
7. Park DK, Kim SD, Lee SH, et al. *Bioresource Tech* 2010; 101: 6151–6156.
8. Alobaid F, Busch J, Stroh A, et al. *J Energ Inst* 2020; 93: 833–846.
9. Konwar K, Nath HP, Bhuyan N, et al. *Fuel* 2019; 256: 115926.

10. Gates BC, Huber GW, Marshall CL, et al. *MRS Bulletin* 2008; 33: 429–435.
11. Meng H, Wang S, Chen L, et al. *Fuel* 2015; 158: 602–611.
12. Aboyade AO. *Thermochemical Acta* 2012; 530.
13. Wang J, Yan Q, Zhao J, et al. *J Thermal Anal Calori* 2014; 118:1663–1673.
14. Di-Nola G, Jong WD and Spliethoff H. *Partition Fuel-Bound Nitro* 2010; 91: 103–115.
15. Guo F, He Y, Hassanpour A, et al. *Energy* 2020; 197: 117147.
16. Toptas A, Yildirim Y, Duman G, et al. *Bioresource Tech* 2015; 177: 328–336.
17. Wang J, Zhang SY, Guo X, et al. *Energy Fuel* 2012; 26(12): 7120–7126.
18. Ullah H, Liu GJ, Yousaf B, et al. *Bioresource Tech* 2017; 245: 73–80.
19. Wang GW, Zhang JL, Shao JG, et al. *Energy Convers Manag* 2016; 124: 414–426.
20. Yu D, Chen MQ, Wei YH, et al. *Powder Technol* 2016; 294: 463–471.
21. Galina NR, Luna CMR, Arce GLAF, et al. *J Energ Inst* 2019; 92(3): 741–754.
22. Guo FH and Zhong ZP. *Environ Pollut* 2018; 239: 21–29.
23. Yelverton TLB, Brashear AT, Nash DG, et al. *Fuel* 2020; 264: 16774.
24. Wang T, Yang Q, Wang Y, et al. *Bioresource Tech* 2020; 297: 122388.
25. Chen X, Xie J, Mei S, et al. *Energies* 2018; 11: 337–350.
26. Zhuang H, He H, Zhao L, et al. *Energ Proced* 2014; 61: 2022–2025.
27. Jaffri GR and Zhang JY. *J Fuel Chem Tech* 2007; 35(2): 128–135.
28. Zhou J, Lin XS, Lin H, et al. *J Fujian Agricult Forestry Univ* 2020; 49: 145–152 (in Chinese).
29. Lin XS, Lin ZX, Lin DM, et al. *J Fujian Coll Forest* 2013; 33: 82–86 (in Chinese).
30. Yan XZ, Chen DL, Liu L, et al. *J Power Eng* 2007; 27(5): 682–686 (in Chinese).
31. Yang YH, Tang YQ and Zhu GJ. *Energ Metal Ind* 2016; 35: 42–44, 52 (in Chinese).